Babol University of Medical Sciences
IJMCM
International Journal of Molecular and Cellular Medicine
p-ISSN: 2251-9637 o-ISSN: 2251-9645
Cellular and Molecular Biology Research Center

In Silico and In vitro Evaluations of the Antibacterial Activities of HIV-1 Nef Peptides against *Pseudomonas aeruginosa*

Eman Koosehlar, Hassan Mohabatkar, Mandana Behbahani*

Department of Biotechnology, Faculty of Biological Science and Technology, University of Isfahan, Isfahan 81746-73441, Iran.

Article type:
Original Article

Received:
2022.11.15
Revised:
2024.05.21
Accepted:
2024.05.29

ABSTRACT

One of the burning issues facing healthcare organizations is multidrug-resistant (MDR) bacteria. *P. aeruginosa* is an MDR opportunistic bacterium responsible for nosocomial and fatal infections in immunosuppressed individuals. According to previous studies, efflux pump activity and biofilm formation are the most common resistance mechanisms in *P. aeruginosa*. The aim of this study was to propose new antimicrobial peptides (AMPs) that target *P. aeruginosa* and can effectively address these resistance mechanisms through *in silico* and *in vitro* assessments. Since AMPs are an attractive alternative to antibiotics, in vitro experiments were carried out along with bioinformatics analyses on 19 Nef peptides (derived from the HIV-1 Nef protein) in the current study. Several servers, including Dbaasps, Antibp2, CLASSAMP2, ToxinPred, dPABBs and ProtParam were used to predict Nef peptides as AMPs. To evaluate the binding affinities, a molecular docking analysis was performed with the HADDOCK web server for all Nef peptide models against two effective proteins of *P. aeruginosa* (MexB and PqsR) that play a role in efflux and quorum sensing. Moreover, the antibacterial and antibiofilm activity of the Nef peptides was investigated in a resistant strain of *P. aeruginosa*. The results of molecular docking revealed that all Nef peptides have a significant binding affinity to the abovementioned proteins. Nef-Peptide-19 has the highest affinity to the active sites of MexB and PqsR with the HADDOCK scores of -136.1 ± 1.7 and -129.4 ± 2, respectively. According to the results of *in vitro* evaluation, Nef peptide 19 showed remarked activity against *P. aeruginosa* with minimum inhibitory and bactericidal concentrations (MIC and MBC) of 10 µM and 20 µM, respectively. In addition, biofilm inhibitory activity was observed at a concentration of 20 µM. Finally, Nef peptide 19 is proposed as a new AMP against *P. aeruginosa*.

Keywords: *Pseudomonas aeruginosa*, antibacterial agents, antimicrobial peptides, molecular docking simulation, biofilms, bacterial infections

Cite this article: Koosehlar E, et al. *In Silico* and *In vitro* Evaluations of the Antibacterial Activities of HIV-1 Nef Peptides against *Pseudomonas Aeruginosa* . *International Journal of Molecular and Cellular Medicine*. 2024; 13(1):46-63. **DOI:** 10.22088/IJMCM.BUMS.13.1.46

*Corresponding: Mandana Behbahani
Address: Department of Biotechnology, Faculty of Biological Science and Technology, University of Isfahan, Iran.
E-mail: Ma_behbahani@yahoo.com

[DOI: 10.22088/IJMCM.BUMS.13.1.46]

Introduction

Nowadays, due to the overuse and misuse of antibiotics, a fundamental challenge for researchers is to discover new therapeutics to counteract emerging bacterial resistance (1). A systematic study (in 2022) estimated that in 2019, 1.27 million deaths occurred in 204 countries due to bacterial resistance (2). According to reports from the World Health Organization (WHO), *P. aeruginosa* is one of the greatest threats to human health (3). The mortality rate in patients with *P. aeruginosa* infections is 18 to 61 percent (4). This bacterium causes an opportunistic nosocomial infection that occurs in cystic fibrosis patients due to the formation of a biofilm in their lungs (5). *P. aeruginosa* is resistant to various antibiotics such as ceftazidime, gentamicin and ciprofloxacin (6). The low permeability of its cell wall, which is 100 times more impermeable than that of *Escherichia coli* (7), the high expression of efflux pumps and biofilm formation are some of the reasons for the resistance of this bacterium (8).

The efflux pump system (EPS) such as mexCD-oprJ, mexXY-oprM, mexEF-oprN and mexAB-oprM play a crucial role in the resistance of *P. aeruginosa* by expelling toxic substances, including antibiotics, from the cell (9) (10). Overexpression of mexAB-oprM leads to a marked development of MDR strains of *P. aeruginosa* (11). EPS consists of three components: the proton motive force (MexB), outer membrane agent (OprM) and periplasmic adhesion protein (MexA) (12). The EPS can be inhibited by interfering with the regulatory mechanism against its overproduction, blocking the pump outlets (OprM), altering the structure of antibiotics and disrupting the assembly of efflux pump autoinducers by EP inhibitors (EPIs). A molecular docking study indicates that some antibiotics act as competitive inhibitors of MexB and determine the active amino acids (10).

Quorum sensing (QS) and biofilm formation are other mechanisms responsible for the adaptability and resistance of *P. aeruginosa* (13). This organism is a typical example of biofilm production (14). QS plays a role in biofilm production and the use of QS inhibitors (QSIs) could be an excellent way to control MDR bacteria (15). The QS systems of *P. aeruginosa* consist of the RhlI/RhIR, LasI/LasR and Pseudomonas quinolone signal (PQS) types (16). PqsR, also known as MvfR (Multiple virulence factor Receptor), is an essential multifunctional receptor in the PQS. Suppression of PqsR disrupts QS signaling and subsequently inhibits the production of virulence factors and biofilm (17). Antimicrobial peptides (AMPs) have been recognized as biofilm suppressors and can reduce the development of resistance (18).

AMPs differ in many ways but have some common features (19). For example, AMPs typically consist of less than 100 amino acids, mainly have an α-helical configuration and are mostly cationic (20). AMPs are inherently amphipathic and hydrophobic, which enables them to interact more strongly with the bacterial membrane (21). Scientists have found AMPs in various organisms (mammals, amphibians, aquatic animals, insects and plants) and microorganisms (protozoa, fungi and bacteria) (22).

More importantly, the researchers have discovered new AMPs in protein sequences of some viruses. For instance, the peptides HBc ARD and pepR are isolated from hepatitis B virus (HBV) and the capsid of Dango virus, respectively (23, 24). Therefore, the current study utilized a bioinformatics approach to investigate 19 peptides from the HIV-1 Nef protein (Nef peptides) for the prediction of antibacterial and antibiofilm activity, estimation of toxicity and half-life, and analysis of molecular interactions. The present study also investigated the inhibitory effect of Nef peptides against *P. aeruginosa* (PTCC 1027) *in vitro*.

[DOI: 10.22088/IJMCM.BUMS.13.1.46]

Materials and methods

The materials and methods of the present study comprised two parts: computational and experimental investigations. The workflow, the different methods used in the current study and the results are summarized in a schematic illustration as a draft of the work (Figure 1).

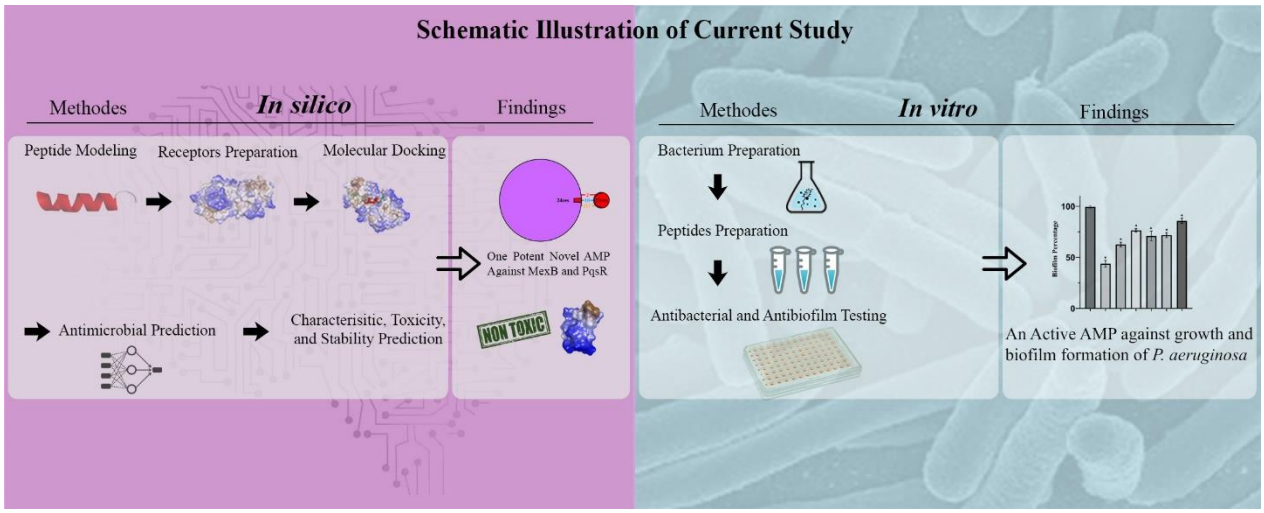

Fig. 1. Illustration of the study workflow.

In silico Studies

3D Structure of Receptors and Nef-Peptides

The 3D structures of the MexB and PqsR proteins were determined from the RCSB database (www.rcsb.org) using PDB ID 6IIA and 4JVD with a resolution of 2.91 and 2.95 Angstroms, respectively. The structures of the Nef peptides were generated from their sequences using *de novo* modeling in the PEP-FOLD$_{3.5}$ server with default parameters (25). The sequences of the Nef peptides are listed in Table 1.

Optimization and Verification of Peptide Models

The best 3D models of the Nef peptides were optimized in 100 steps using the steepest descent algorithm of the Chimera software (version 1.15) (26). Finally, the PDB files of the optimized peptides were uploaded to PROCHECK and ProSA to check Ramachandran plots and Z-score numbers, respectively (27, 28).

Antimicrobial and Antibiofilm Prediction of Nef-Peptides

The Nef peptide sequences were screened for antimicrobial activity using three prediction web servers, including CLASSAMP2 (29), Antibp2 (30), and Dbaasps (31). The dPABBs web server was also used to predict antibiofilm activity (32). Each peptide was scored based on the probability of predicted antimicrobial properties. These servers use a variety of training datasets for machine-learning approaches. Various algorithms were used, including Random Forest (RF), Discriminate Analysis (DA), Support Vector Machine (SVM) and Artificial Neural Network (ANN) (29, 33).

Physicochemical Properties prediction

ProtParam was used to predict critical indices such as GRAVY (34), amphiphilicity, net charge, net hydrogen, and molecular weight. Based on the amino acid composition of each peptide sequence, the

[DOI: 10.22088/IJMCM.BUMS.13.1.46]

dPABBs web server predicts the physicochemical properties of each query (32). Furthermore, the percentage of secondary structure in the Nef peptides was analyzed using YASARA software (version 21.12.19) (35).

Table 1. The sequences of all 19 Nef peptides.

Nef-Peptides	Sequences
Nef-Peptide-1	GGKWSKSSVVGWPTVRERMR
Nef-Peptide-2	GWPTVRERMRRAEPAADGVG
Nef-Peptide-3	RAEPAADGVGAASRDLEKHG
Nef-Peptide-4	AASRDLEKHGAITSSNTAAT
Nef-Peptide-5	AITSSNTAATNAACAWLEAQ
Nef-Peptide-6	NAACAWLEAQEEEEVGFPV T
Nef-Peptide-7	EEEEVGFPVTPQVPLRPMTY
Nef-Peptide-8	KAAVDLSHFLKEKGGLEGLI
Nef-Peptide-9	KEKGGLEGLIHSQRRQDILD
Nef-Peptide-10	HSQRRQDILDLWIYHTQGYF
Nef-Peptide-11	LWIYHTQGYFPDWQNYTPGP
Nef-Peptide-12	PDWQNYTPGPGVRYPLTFGW
Nef-Peptide-13	GVRYPLTFGWCYKLVPVEPD
Nef-Peptide-14	CYKLVPVEPDKVEEANKGEN
Nef-Peptide-15	KVEEANKGENTSLLHPVSLH
Nef-Peptide-16	TSLLHPVSLHGMDDPEREVL
Nef-Peptide-17	GMDDPEREVLEWRFDSRLAF
Nef-Peptide-18	EWRFDSRLAFHHVARELHPE
Nef-Peptide-19	HHVARELHPEYFKNC

Toxicity and Stability Estimation

The peptide sequences were checked using the online tools ToxinPred and ProtParam to predict the instability index, half-life and toxicity in mammalian cells (30, 34).

Molecular Docking Analysis

Molecular docking was performed using the HADDOCK web server (HADDOCK2.4) (36, 37), and 19 Nef peptides were docked to MexB and PqsR proteins. The peptides were considered as ligands (labeled in chain B), and MexB and PqsR proteins were selected as receptors (labeled in chain A). Docking was performed with optimized parameters for the peptide-protein complex. For the sampling parameters, the number of structures for rigid body docking was set to 1000, the number of structures for semi-flexible refinement was set to 200, the cutoff parameter for RMSD was set to 5 and water was selected as the explicit solvent.

Peptide-Protein Complex Interaction Analysis

The Discovery Studio Visualizer software and the PDBsum tool were used to analyze the peptide-protein complexes and display the binding residues (38, 39).

***In vitro* Studies**

Bacterium Strain and Nef-Peptide Preparation

[DOI: 10.22088/IJMCM.BUMS.13.1.46]

P. aeruginosa (PTCC 1074), also known as ATCC 9027, was obtained from Iranian Research Organization for Science and Technology (IROST), Tehran, Iran. This species was cultured in nutrient broth and agar (NB and NA) for 24 hours at 37 °C, stored at four °C and recultured for subsequent studies. The nineteen Nef peptides were purchased from the Cenetr for AIDS Reagents, National Institute for Biological Standards and Control (NIBSC), UK (with repository reference ARP7074). The solution of Nef peptides was prepared in deionized water at a concentration of 2560 µM based on their molecular weight.

Antibacterial Susceptibility Testing

A 0.5 McFarland turbidity standard (1.5×10^8) was prepared from overnight cultured *P. aeruginosa* PTCC 1074, and added to 96-well microplates (SPL Life Sciences, South Korea). In addition, antibacterial susceptibility was performed and evaluated using the minimum inhibitory concentration (MIC) method. In brief, 100 µl of Nef peptides, 100 µl of NB medium and 50 µl of bacterial suspension were added to each well. The bacterial suspension and NB medium were positive and negative controls, respectively. The lowest concentration at which no growth was seen after overnight incubation at 37 °C was considered the MIC.

Furthermore, the MBC method was used to test bactericidal activity. Ten µl of the wells in which the MIC was observed and 2-fold of the MIC were transferred to a NA and incubated at 37 °C for 24 hours. The MBC is the lowest concentration at which no bacterial colonies form on the NA (40). All tests were done in triplicate.

Antibiofilm Inhibition Evaluation

Biofilm formation was determined using the microtiter plate method to investigate the efficacy of the Nef peptides (41, 42). The *P. aeruginosa* PTCC 1074 suspension was incubated overnight for 48 hours at 37 °C with 20 µM of the best Nef peptides (Nef peptide-1, Nef peptide-10, Nef peptide-14, Nef peptide-16, Nef peptide-18 and Nef peptide-19) in 48-well microplates (SPL Life Sciences, South Korea). After incubation, the microplates were washed with physiological saline to remove the unbound and dead cells and allowed to dry at room temperature for 10 minutes. Then, they were stained by adding 250 µL of 0.1% crystal violet solution for 10 minutes and stored at room temperature to dry and stabilize the biofilm. Finally, 200 µL of 95% ethanol was added for 10 minutes and the qualification of biofilm production was measured using a microplate reader (Awareness Technology ChroMate® Microplate Reader, America) at OD_{595nm}.

Statistical Analysis

The data of treated groups and control were compared by two-way ANOVA with a *p*-value of less than 0.05. These statistical analyses were performed using GraphPad Prism software (version 9.3.1.471, San Diego, CA, USA). All tests were carried out in triplicate, and results were presented as mean ± SD.

Results

Computational Analysis

Nef-Peptide 3D Structure Prediction and Verification

Prediction of the 3D structures of Nef peptides by PEPFOLD3.5 yielded ten models for each Nef peptide. The PEPFOLD model1 for all Nef peptides was found to be as the best model with the more negative sOPEP (Optimized Potential for Efficient Structure Prediction) energy. The final selected Nef

[DOI: 10.22088/IJMCM.BUMS.13.1.46]

peptide models had sOPEP energy ranging from -34.003 to -15.9598. In addition, the template modeling (TM) values of the Nef peptides models ranged from 0.186 to 0.642 (Table 2). TM scores above 0.5 to 1 were considered perfect, and scores below 0.17 were considered generally weak. The Z-score and Ramachandran plot statics of all optimized Nef peptide models were within an acceptable region (Table 2).

Table 2. Outputs of the structural models of the Nef peptides from PEP-FOLD3.5, PROCHECK and ProSA web servers.

Nef-Peptides	sOPEP	TM Score	Residues in most favored regions (%)	Residues in Additional allowed regions (%)	Residues in disallowed regions (%)	Z-score
Nef-Peptide-1	23.8396	0.377	86/7	13/3	0	-0.53
Nef-Peptide-2	25.4893	0.528	86/7	13/3	0	-1/40
Nef-Peptide-3	21.7697	0.449	86/7	13/3	0	-1/35
Nef-Peptide-4	18.1814	0.384	82/4	17/6	0	-1/16
Nef-Peptide-5	24.3305	0.520	100	0	0	-0/9
Nef-Peptide-6	31.9092	0.619	100	0	0	-1/03
Nef-Peptide-7	15.9598	0.273	92/3	7/7	0	-0/1
Nef-Peptide-8	31.7345	0.407	86/7	13/3	0	-1/03
Nef-Peptide-9	24.426	0.617	86/7	13/3	0	-0/81
Nef-Peptide-10	34.003	0.599	88/2	11/8	0	-1/75
Nef-Peptide-11	26.1485	0.217	92/9	7/1	0	-0/1
Nef-Peptide-12	25.4436	0.186	50	50	0	-0/63
Nef-Peptide-13	22.6902	0.226	85/7	14/3	0	-0/34
Nef-Peptide-14	26.5359	0.428	93/3	6/7	0	-1/37
Nef-Peptide-15	20.6712	0.378	81/2	18/8	0	-2/4
Nef-Peptide-16	16.8204	0.317	66/7	33/3	0	-1/81
Nef-Peptide-17	27.9416	0.340	70/6	29/4	0	-0/39
Nef-Peptide-18	30.7537	0.555	88/2	11/8	0	-0/96
Nef-Peptide-19	20.4103	0.642	91/7	8/3	0	-1/61

According to PROCHECK results, 91.7% of Nef peptide-19 residues were in the most preferred region, 8.3% were in additional allowed regions, and no residues were in disallowed regions. Cross-validation by ProSA also indicated that all PEPFOLD models had a Z-score in the negative range and within the range of experimentally validated proteins (Table 2); therefore, they were considered accurate (27, 28).

The Ramachandran and Z-score plots of the Nef-Peptide-19 model are illustrated in Figures 2a and 2b, respectively. Nef peptide-19 has a Z-score of -1.61 (within the experimentally validated regions), 11 amino acid residues in the preferred regions and none in the disallowed regions.

AMP Prediction

The antimicrobial activity of all Nef peptides was predicted using three AMP predictor web servers: AntiBP2, ClassAMP, and Dbaasps. These web servers utilize full residue analysis to predict antimicrobial properties using machine learning algorithms. The results are annotated in terms of antibacterial, antiviral and antifungal activities. However, the present study focused on antibacterial activity. Based on the results,

[DOI: 10.22088/IJMCM.BUMS.13.1.46]

except Nef peptide-3, Nef peptide-9, Nef peptide-14, and Nef peptide-15, all other Nef peptides were predicted to be AMPs by at least one of the servers (Table 3).

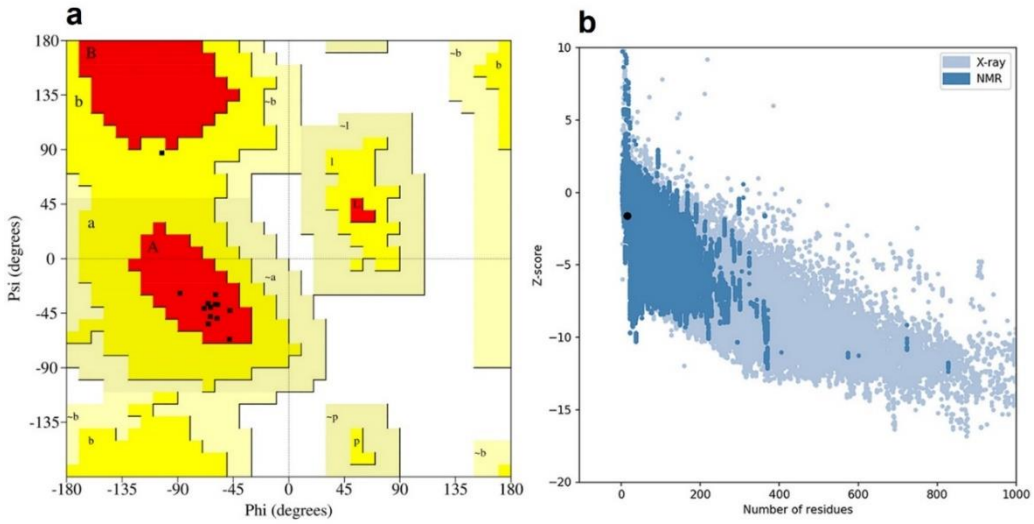

Fig. 2. a) Ramachandran plot for Nef-Peptide-19. Nef-Peptide-19 has 11 amino acid residues in the preferred regions and none in the disallowed regions. b) Nef-Peptide-19 has a z-score of −1.61 and is within the experimentally validated regions.

Table 3. Antimicrobial prediction results using AntiBP2, ClassAMP and Dbaasps web servers.

Nef-Peptides	AntiBP2	ClassAMP (RF)	ClassAMP (SVM)	Dbaasps	Properties
Nef-Peptide-1	No	Antibacterial	Antifungal	Yes	Antimicrobial activities
Nef-Peptide-2	No	Antibacterial	Antiviral	No	
Nef-Peptide-3	No	Antifungal	Antifungal	No	
Nef-Peptide-4	No	Antibacterial	Antiviral	No	
Nef-Peptide-5	Antibacterial	Antibacterial	Antiviral	No	
Nef-Peptide-6	No	Antibacterial	Antifungal	No	
Nef-Peptide-7	No	Antibacterial	Antifungal	No	
Nef-Peptide-8	Antibacterial	Antibacterial	Antifungal	No	
Nef-Peptide-9	No	Antifungal	Antifungal	No	
Nef-Peptide-10	No	Antibacterial	Antiviral	No	
Nef-Peptide-11	No	Antibacterial	Antifungal	No	
Nef-Peptide-12	No	Antibacterial	Antiviral	No	
Nef-Peptide-13	No	Antibacterial	Antifungal	No	
Nef-Peptide-14	No	Antifungal	Antifungal	No	
Nef-Peptide-15	No	Antiviral	Antifungal	No	
Nef-Peptide-16	No	Antibacterial	Antibacterial	No	
Nef-Peptide-17	No	Antibacterial	Antifungal	No	
Nef-Peptide-18	No	Antibacterial	Antifungal	No	
Nef-Peptide-19	No	Antibacterial	Antifungal	No	

Note; Yes means AMP, and No implies non-AMP.

[DOI: 10.22088/IJMCM.BUMS.13.1.46]

Nef-Peptide Physiochemical Properties

The prediction of the physicochemical properties of the Nef peptides showed different values for the net charge (from -5 to +4 for Nef-peptide-6 and Nef-peptide-1, respectively), the hydropathicity index (between -1.13 and 0.24) and the amphipathicity index (higher than 0.8 for Nef peptide-1, Nef peptide-9, Nef peptide-14, Nef peptide-18 and Nef peptide-19) (43) (Table 4).

Table 4. Physicochemical properties of the Nef peptides predicted with the dPABBs web server.

Nef-Peptides	Hydropathicity	Amphiphilicity	Net Hydrogen	Charge	pI	MW
Nef-Peptide-1	-0.90	0.80	1.15	4.00	11.73	2303.96
Nef-Peptide-2	-0.94	0.62	1.05	1.00	9.80	2211.76
Nef-Peptide-3	-0.84	0.63	0.80	-0.50	5.50	2007.42
Nef-Peptide-4	-0.48	0.44	0.85	0.50	7.10	2001.41
Nef-Peptide-5	0.24	0.13	0.65	-1.00	4.00	1994.43
Nef-Peptide-6	-0.17	0.38	0.55	-5.00	3.52	2193.65
Nef-Peptide-7	-0.52	0.44	0.65	-3.00	4.10	2318.92
Nef-Peptide-8	0.14	0.75	0.55	0.50	7.10	2125.81
Nef-Peptide-9	-1.13	0.94	1.10	0.50	7.11	2292.90
Nef-Peptide-10	-0.94	0.58	1.15	1.00	7.25	2577.17
Nef-Peptide-11	-0.94	0.20	0.75	-0.50	5.09	2484.03
Nef-Peptide-12	-0.88	0.18	0.75	0.00	6.18	2351.90
Nef-Peptide-13	0.02	0.37	0.60	0.00	6.38	2340.03
Nef-Peptide-14	-1.02	0.80	0.80	-2.00	4.59	2261.82
Nef-Peptide-15	-0.72	0.70	0.80	0.00	6.05	2202.76
Nef-Peptide-16	-0.27	0.39	0.65	-2.00	4.73	2245.84
Nef-Peptide-17	-0.85	0.56	1.00	-3.00	4.30	2469.00
Nef-Peptide-18	-0.97	0.78	1.05	0.50	6.31	2533.09
Nef-Peptide-19	-1.09	0.87	0.93	1.50	7.31	1880.33

Prediction of the secondary structure of Nef peptides using YASARA software indicated that 86.7% of the conformation of Nef peptide19 was α-helix (Table 5). The α-helix structure is the preferred conformation in AMPs and is better able to fit into the membrane (44).

Molecular Docking Analysis

The results of the molecular docking study for the two target proteins MexB and PqsR with the 19 Nef peptides are presented in Tables 7 and 8, respectively. The HADDOCK results of the MexB protein with the 19 Nef peptides showed that Nef-Peptide-19 has the highest HADDOCK score of −136.1, with a Z-score of −1.6 and an RMSD of 0.6 at the DBP active site (Table 6). HADDOCK grouped 128 structures into 13 clusters, describing 64 % of the generated water-refined models.

The HADDOCK results of PqsR with Nef peptides demonstrated that Nef peptide-19 yielded the highest HADDOCK score of -129.4 ± 2.9, with a Z-score of −1.3 and an RMSD of 0.3 at the active site of PqsR's (Table 7). HADDOCK clustered 185 structures in 4 clusters, corresponding to 92% of the generated water-refined HADDOCK models.

Peptide-Protein Complex Interaction Analysis

[DOI: 10.22088/IJMCM.BUMS.13.1.46]

Table 5. Content of the secondary structure with the YASARA software. 86.7% of the Nef peptide-19 structure is α-helix.

Nef-Peptides	α-Helix (%)	Random Coil (%)	β Turn (%)	β Sheet (%)
Nef-Peptide-1	35	65	00	00
Nef-Peptide-2	65	35	00	00
Nef-Peptide-3	45	35	20	00
Nef-Peptide-4	40	60	00	00
Nef-Peptide-5	65	35	00	00
Nef-Peptide-6	80	20	00	00
Nef-Peptide-7	30	50	20	00
Nef-Peptide-8	60	20	20	00
Nef-Peptide-9	65	35	00	00
Nef-Peptide-10	75	25	00	00
Nef-Peptide-11	00	60	40	00
Nef-Peptide-12	00	80	20	00
Nef-Peptide-13	00	80	20	00
Nef-Peptide-14	50	50	00	00
Nef-Peptide-15	55	25	20	00
Nef-Peptide-16	30	50	20	00
Nef-Peptide-17	40	40	20	00
Nef-Peptide-18	70	30	00	00
Nef-Peptide-19	86.7	13.3	00	00

Table 6. Nef peptides HADDOCK 2.4 results interacting with MexB protein of *P. aeruginosa*.

Nef-Peptides	HADDOCK score	CLUSTER SIZE	RMSD	VW energy	Electrostatic energy	Desolvation energy	Restraints violation energy	BSA	Z-Score
Nef-Peptide-1	-76.0 ± 1.5	16	5.9 ± 0.1	-56.5 ± 4.3	-183.5 ± 38.6	-7.7 ± 2.5	248.4 ± 48.7	1756.5 ± 29.4	-1.8
Nef-Peptide-2	-82.8 ± 7.1	8	0.3 ± 0.2	-57.4 ± 4.4	-227.8 ± 33.6	4.4 ± 1.6	158.6 ± 48.6	1820.0 ± 41.3	-2.6
Nef-Peptide-3	-72.5 ± 6.1	16	4.4 ± 0.0	-47.9 ± 2.8	-206.8 ± 29.7	-5.5 ± 2.1	222.0 ± 11.2	1645.3 ± 30.9	-2.0
Nef-Peptide-4	-70.6 ± 5.0	19	4.5 ± 0.1	-48.6 ± 7.9	-253.3 ± 50.0	10.0 ± 3.5	186.2 ± 54.4	1673.5 ± 39.5	-2.0
Nef-Peptide-5	-77/3	12	1/0± 0/1	-63/2 ± 5/0	-97/8 ± 4/5	-10/7 ± 1/5	161/4 ± 32/2	1607/8 ± 105/2	-1/6
Nef-Peptide-6	-104.2 ± 6.4	14	0.6 ± 0.0	-66.1 ± 2.6	-210.7 ± 34.6	-11.2 ± 2.8	152.2 ± 10.8	2134.5 ± 43.8	-2.2
Nef-Peptide-7	-89.7 ± 4.2	19	1.5 ± 0.1	-64.1 ± 3.9	-259.1 ± 5.2	1.4 ± 3.2	248.8 ± 78.3	1996.1 ± 52.5	-1.8

[DOI: 10.22088/IJMCM.BUMS.13.1.46]

Nef-Peptide-8	-83.9 ± 5.1	31	0.3 ± 0.2	-63.9 ± 6.0	-187.9 ± 35.6	-2.9 ± 2.5	205.4 ± 43.5	1762.8 ± 86.0	-2.2
Nef-Peptide-9	-83.5 ± 6.4	7	6.1 ± 0.1	-57.5 ± 3.0	-292.5 ± 58.5	14.4 ± 4.6	181.1 ± 39.5	2005.4 ± 125.2	-2.0
Nef-Peptide-10	-93.4 ± 5.2	18	0.9 ± 0.0	-59.7 ± 6.2	-237.2 ± 37.4	-12.8 ± 0.6	266.2 ± 43.2	1848.9 ± 46.7	-1.3
Nef-Peptide-11	-92.6± 9.4	10	0.3 ± 0.2	-78.2 ± 3.3	-105.5 ± 17.9	-28.2 ± 6.6	348.9 ± 49.0	2027.1 ± 63.8	-1.9
Nef-Peptide-12	-83.9 ± 1.2	8	1.5 ± 0.0	-74.5 ± 4.0	-102.8 ± 11.2	-8.6 ± 0.9	197.0 ± 60.2	1737.7 ± 18.6	-1.8
Nef-Peptide-13	-96.1 ± 10.2	27	0.3 ± 0.2	-76.6 ± 2.4	-93.9 ± 14.8	-25.3 ± 3.1	245.6 ± 80.3	1870.5 ± 31.5	-2.0
Nef-Peptide-14	-111.8 ± 2.6	12	0.5 ± 0.3	-76.3 ± 2.6	-279.9 ± 27.4	6.7 ± 1.2	138.1 ± 23.1	2174.1 ± 28.1	-2.8
Nef-Peptide-15	-76.6 ± 1.6	27	0.8 ± 0.2	-64.1 ± 2.3	-109.1 ± 17.4	-9.6 ± 1.3	189.8 ± 45.2	1970.6 ± 122.8	-1.7
Nef-Peptide-16	-87.0 ± 5.5	11	0.3 ± 0.2	-60.9 ± 6.9	-203.6 ± 50.3	-11.9 ± 3.4	265.4 ± 63.8	1806.6 ± 99.3	-1.3
Nef-Peptide-17	-102.0± 4.9	17	1.8 ± 0.0	-83.1 ± 3.6	-153.1 ± 32.1	-7.8 ± 1.7	195.5 ± 20.7	2035.1 ± 49.9	-1.6
Nef-Peptide-18	-124.5± 3.4	33	0.3 ± 0.2	-61.0 ± 4.5	-335.9 ± 42.0	-12.3 ± 5.2	159.9 ± 51.4	2085.7 ± 31.7	-2.6
Nef-Peptide-19	-136.1± 1.7	20	0.6 ± 0.3	-74.9 ± 4.2	-258.5 ± 27.9	-9.5 ± 1.0	189.6 ± 58.4	1668.6 ± 61.0	-1.9

Note, RMSD: Root Mean Square Deviation, VW energy: Van der Waals energy, BSA: Buried Surface Area

Table 7. Nef peptides HADDOCK 2.4 results interacting with the PqsR protein of *P. aeruginosa.*

Nef-Peptides	HADDOCK score	Cluster size	RMSD	VW energy	Electrostatic energy	Desolvation energy	Restraints violation energy	BSA	Z-Score
Nef-Peptide-1	-91.6 ± 11.3	8	0.7 ± 0.4	-49.5 ± 8.3	-117.8 ± 30.8	-25.2 ± 1.6	67.3 ± 17.5	67.3 ± 17.5	-1.6
Nef-Peptide-2	-78.9 ± 3.9	101	0.6 ± 0.4	-31.8 ± 3.1	-223.4 ± 28.6	-10.6 ± 2.1	82.1 ± 27.7	1344.2 ± 50.2	-1.3
Nef-Peptide-3	-80.3 ± 1.8	95	0.2 ± 0.1	-53.2 ± 3.8	-106.8 ± 4.8	-14.4 ± 1.3	86.0 ± 31.0	1662.8 ± 51.1	-2.2
Nef-Peptide-4	-86.2 ± 3.5	42	0.4 ± 0.2	-41.6 ± 1.8	-265.6 ± 16.2	0.0 ± 1.7	84.5 ± 24.3	1486.7 ± 66.6	-2.7
Nef-Peptide-5	-79.0 ± 0.9	56	3.4 ± 0.3	-59.0 ± 5.0	-87.2 ± 13.4	-14.3 ± 3.0	116.9 ± 5.6	1559.6 ± 86.0	-1.8
Nef-Peptide-6	-79.0 ± 0.9	56	3.4 ± 0.3	-59.0 ± 5.0	-87.2 ± 13.4	-14.3 ± 3.0	116.9 ± 5.6	1559.6 ± 86.0	-1.8
Nef-Peptide-7	-71.6 ± 2.8	6	2.7 ± 0.0	-42.5 ± 3.1	-144.0 ± 23.1	-10.9 ± 1.2	105.7 ± 22.2	1534.8 ± 34.3	-1.8

[DOI: 10.22088/IJMCM.BUMS.13.1.46]

Nef-Peptide-8	-72.5 ± 3.8	16	0.9 ± 0.3	-31.4 ± 3.2	-211.8 ± 40.5	-5.5 ± 4.3	67.9 ± 17.4	1344.9 ± 41.4	-1.8
Nef-Peptide-9	-78.1 ± 3.5	33	0.8 ± 0.5	-32.1 ± 5.6	-304.3 ± 21.6	3.4 ± 1.6	115.3 ± 24.2	1566.8 ± 84.9	-1.2
Nef-Peptide-10	-123.4 ± 7.5	109	0.3 ± 0.2	-58.6 ± 3.4	-191.1 ± 9.9	-35.9 ± 2.3	92.6 ± 24.9	1695.9 ± 69.4	-2.1
Nef-Peptide-11	-95.4 ± 3.2	48	0.3 ± 0.2	-53.1 ± 4.0	-110.8 ± 14.6	-27.9 ± 2.1	77.7 ± 21.1	1618.4 ± 27.8	-2.1
Nef-Peptide-12	-100.2 ± 5.1	52	0.4 ± 0.2	-65.0 ± 3.9	-78.8 ± 17.9	-24.9 ± 3.1	54.7 ± 29.8	1652.7 ± 87.0	-2.3
Nef-Peptide-13	-101.2 ± 2.2	10	0.6 ± 0.4	-58.6 ± 7.5	-120.1 ± 43.3	-27.9 ± 2.2	94.0 ± 15.4	1742.5 ± 78.1	-1.6
Nef-Peptide-14	-67.0 ± 7.6	23	0.9 ± 0.8	-49.2 ± 2.7	-107.5 ± 38.7	-6.2 ± 3.1	99.2 ± 30.4	1457.3 ± 49.7	-1.6
Nef-Peptide-15	-90.5 ± 1.5	75	0.3 ± 0.2	-45.7 ± 1.4	-216.9 ± 18.4	-13.8 ± 1.3	123.5 ± 25.0	1606.9 ± 72.2	-1.8
Nef-Peptide-16	-96.6 ± 7.6	34	0.4 ± 0.3	-50.9 ± 4.0	-212.5 ± 22.1	-9.0 ± 0.8	59.0 ± 12.8	1716.9 ± 27.9	-2.3
Nef-Peptide-17	-83.9 ± 4.6	16	0.4 ± 0.2	-41.8 ± 3.2	-195.7 ± 7.0	-9.7 ± 1.7	67.7 ± 31.5	1548.7 ± 34.3	-1.7
Nef-Peptide-18	-112.5± 2.1	95	0.3 ± 0.2	-59.5 ± 7.8	-134.7 ± 29.5	-33.9 ± 3.9	79.0 ± 28.1	1778.8 ± 24.6	-2.5
Nef-Peptide-19	-129.4 ± 2.9	62	0.3 ± 0.3	-46.6 ± 7.3	-280.7 ± 15.9	-25.8 ± 3.4	17.9 ± 16.4	1486.2 ± 35.5	-1.3

The complex analysis of MexB protein with Nef peptide-19 indicated that 24 residues of MexB binding site interacted with 13 residues of Nef peptide-19. The PDBsum results revealed two ionic, ten hydrogenic and 117 van der Waals interactions in the peptide-protein complex (Figure 3a). The 3D interactions of the MexB binding pocket were illustrated in Discovery Studio (Figure 3b). Among these amino acids, R128, D174, Q176, S180 and D760 of the active site of vital MexB bonded with the residues of Nef peptide-19. Furthermore, H2 and V3 of Nef peptide-19 were in contact with 6 and 4 residues of the active site of MexB, respectively (Figure 3c). Therefore, these two residues of Nef peptide-19 are essential for suppressing MexB protein.

Complex analysis of the active sites of Nef peptide-19 and MexB revealed 129 interactions: two ionic, ten hydrogenic and 117 van der Waals interactions. The critical residues of the active site of MexB (R128, D174, Q176, S180, D760) were involved in hydrogen bonds with Nef peptide-19 residues.

Docking analysis of the PqsR protein and Nef peptide-19 showed that 12 residues of Nef peptide-19 were bound to the 19 residues of the PqsR active site through 120 interactions (two were ionically bound, 10 were hydrogen bonded, and 108 were not bound) (Figure 4a).

The 3D interactions of the PqsR binding pocket were visualized in Discovery Studio (Figure 4b). Among these residues, seven of the essential amino acids of the active site of PqsR, I149, I186, L189, L207, I236, Y258, and T265 (45), were suppressed by the residues of Nef peptide-19 (Figure 4c).

[DOI: 10.22088/IJMCM.BUMS.13.1.46]

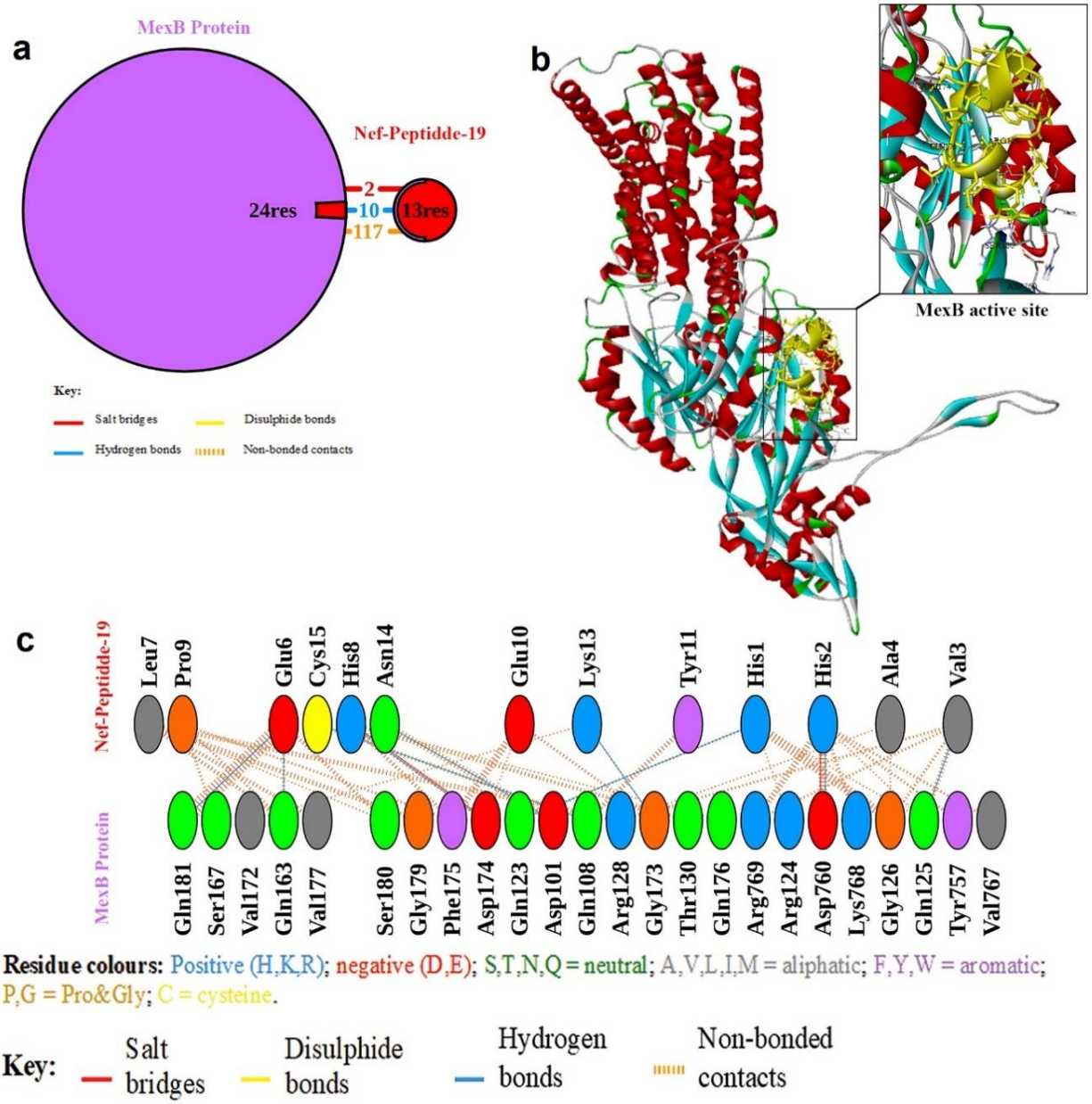

Fig. 3. Analysis of the MexB_Nef peptide-19 complex. **a** Schematic representation of the MexB binding pocket and the Nef peptide-19 complex. **b** Crystal structure of MexB (PDB: 6IIA) bound to Nef-Peptide-19 (yellow). **c** 2D diagram of the interactions between Nef peptide-19 and MexB.

Analysis of *in vitro* evaluations

Assessment of Antibacterial Activity

The results of antibacterial evaluation of Nef peptides against *P. aeruginosa* (PTCC 1074) revealed that six Nef peptides had significant MIC values, as shown in Table 8. Among them, Nef-Peptide-19 was

[DOI: 10.22088/IJMCM.BUMS.13.1.46]

the most effective peptide, with MIC and MBC values of 10 µM (18.8 µg/mL) and 20 µM (37.6 µg/mL), respectively.

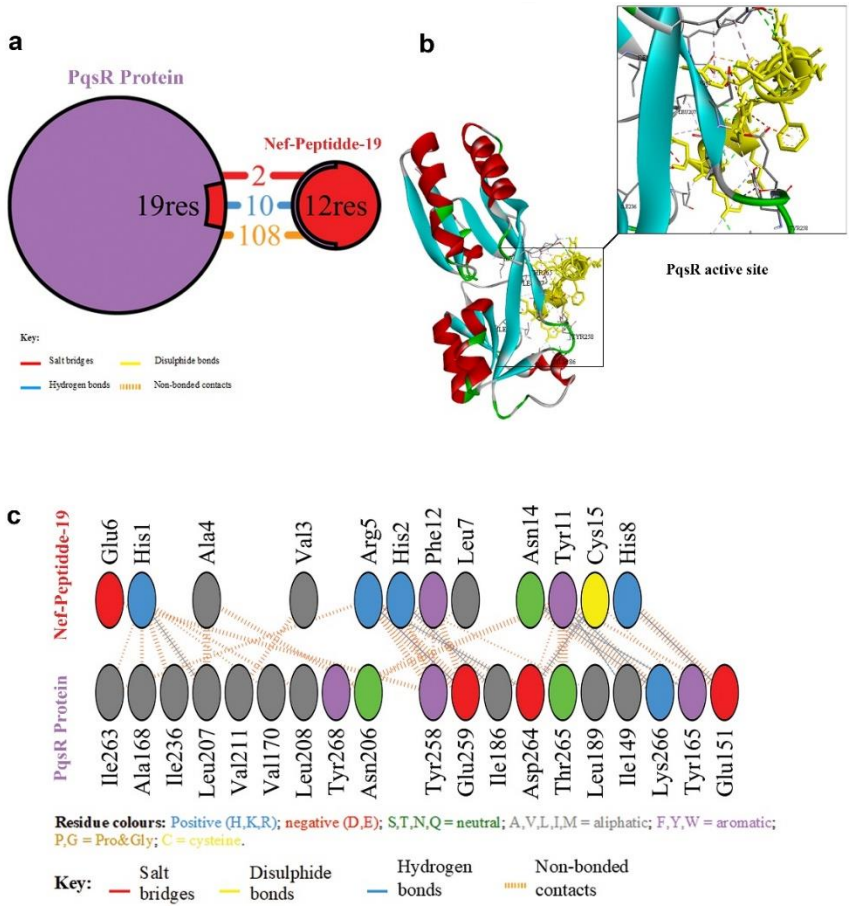

Fig. 4. Analysis of the interactions between PqsR and Nef peptide-19. a) Schematic representation of the PqsR binding site with the Nef peptide-19 complex. b) Crystal structure of PqsR (PDB: 4JVD) bound to Nef peptide-19 (yellow). **c** 2D diagram of the Nef peptide-19 and PqsR interactionsL.

Table 8. Antibacterial activities of the best Nef peptides by MIC test.

Nef-Peptides	MIC values (µM)
Nef-Peptide-1	20 (37.6 µg/mL)
Nef-Peptide-10	20 (37.6 µg/mL)
Nef-Peptide-14	20 (37.6 µg/mL)
Nef-Peptide-16	20 (37.6 µg/mL)
Nef-Peptide-18	20 (37.6 µg/mL)
Nef-Peptide-19	10 (18.8 µg/mL)

Assessment of Antibiofilm Activity

Antibiofilm evaluation of the top six Nef peptides against *P. aeruginosa* (PTCC 1074) showed that Nef peptide-19 was the most active peptide. The percentage inhibitory effect of Nef peptide-19 on biofilm formation was 56.23 at the concentration of 20 µM (37.6 µg/mL). All antibiofilm activities of Nef peptides are demonstrated in Figure 5.

[DOI: 10.22088/IJMCM.BUMS.13.1.46]

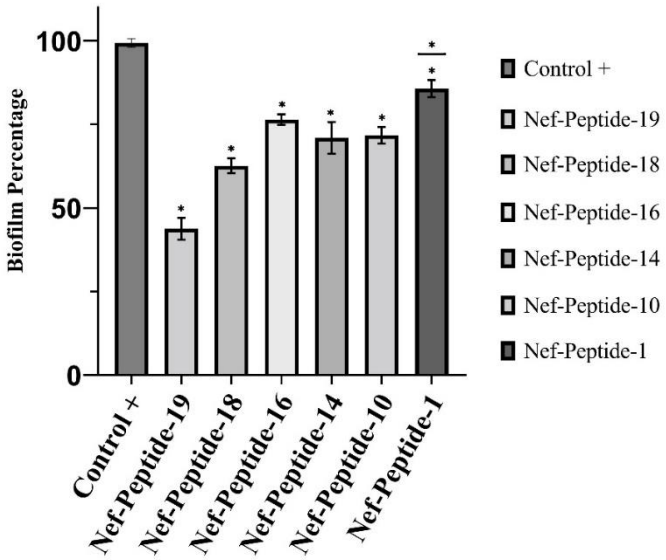

Fig. 5. The percentage of biofilm formation of P.aeruginosa in the presence of the top six Nef peptides at 20 µM. Values were presented as mean and standard deviation (±SD) from triplicate independent assays (two-way ANOVA, P-value<0.05).

Discussion

The increase in MDR bacteria has led to a decrease in the efficacy of conventional antibiotics in recent years (46). *P. aeruginosa* is already resistant to various antibiotics, including ciprofloxacin, gentamicin, imipenem, fluoroquinolone, and ceftazidime (47). The use of AMPs instead of conventional antibiotics has been considered a new strategy to combat MDR bacteria (48). Researchers have recently focused on viral-derived peptides to assess their antimicrobial activity. For instance, pepR (isolated from the dengue virus capsid protein) is active against *Staphylococcus aureus* biofilms (49), M2 AH (isolated from the influenza virus M2 protein) is active against influenza virus infections (50), and P24-derived peptides (isolated from the HIV-1 virus P24 protein) are active against the HIV-1 virus (51).

New AMPs can be developed by using evolved prediction tools that search the protein sequences of different organisms (52). Some peptides derived from HIV-1 proteins, such as gp41, gp120 and p24, have been investigated for their potential as antimicrobial agents (51, 53). In the current study, bioinformatics and laboratory techniques were used to assess the antimicrobial activities of 19 peptides from the HIV-1 Nef protein against *P. aeruginosa*. To our knowledge, HIV-1 Nef peptides had moderate to strong antibacterial activities against *P. aeruginosa*.

Moreover, in the present study, 19 Nef peptides with two pathogenic proteins (MexB and PqsR) were docked via HADDOCK. The 2021 study by Dong et al. on the MexB protein revealed that targeting MexB with the BING peptide (isolated from *Oryzias latipes*) sensitizes MDR bacteria, including *P. aeruginosa*, to antibiotics (54). The molecular docking results of the current study showed that Nef peptide-19 fitted into the binding site MexB via several residues, including two crucial residues in DBP, R128 and S180 (10, 55) with a HADDOCK score of -136.1 ± 1.7. Compounds with a molecular mass greater than 1000 (such as Nef Peptide-19) can bind to the DBP of MexB and disrupt EPS function (55). PqsR is another pathogenic

[DOI: 10.22088/IJMCM.BUMS.13.1.46]

protein of *P. aeruginosa* that has been described in previous studies as a potential target for disrupting the QS system and reducing the expression of several virulence factors (56, 57). Our docking analysis revealed that Nef peptide-19 has the highest affinity for the PqsR binding site and contacts key residues such as I149, I186, L189, L207, L208, I236, Y258 and T268 (45, 58) with a HADDOCK score of -129.4 ± 2.9.

Several AMPs have been studied *in vitro* to suppress *P. aeruginosa* infections (59, 60). In 2020, Li et al. reported the antibacterial activity of CM4, a cationic AMP from the silkworm *Bombyx mori*, against *P. aeruginosa* with an MIC value of 18 µM (61). 6K-F17, a peptide synthesized by Beaudoin et al. in 2018, showed MIC values of 2-256 µg/ml against several species of *P. aeruginosa* (62). Compared to the reported results, Nef peptide-19 showed considerable bacteriostatic and bactericidal activities against *P. aeruginosa* with MIC and MBC values of 10 µM (18.8 µg/ml) and 20 µM (37.6 µg/ml), respectively. In 2022, Aflakian et al. suggested that three novel synthesized AMPs (WSF, FASK, YDVD) at a concentration of 800 µg/ml could inhibit the biofilm production of *P. aeruginosa* (63). Furthermore, Gopal et al. reported in 2013 that NRC-16 affects the production of *P. aeruginosa* from 2.17 to 17.4 µg/ml (64). The results of the ongoing study revealed that Nef peptide-19 at a concentration of 20 µM (37.6 µg/ml) was able to inhibit 53.23% of biofilm formation. Based on these results, we hypothesize that Nef peptide-19 could be a potential new AMP to fight bacterial infections.

In order to advance the development of Nef peptides as potential therapeutics against P. aeruginosa, certain limitations need to be addressed in future research. These could include evaluating the efficacy of Nef peptides against a broader range of clinical isolates, assessing their antibacterial and antibiofilm activities using an in vivo model, and testing the stability of the AMPs under physiological conditions to ensure their safety.

Acknowledgments

The authors would like to thank the University of Isfahan for supporting this study.

Ethical considerations

This research was financially supported by the University of Isfahan [grant number UI14010310]. This article does not include studies with human participants or animals conducted by any of the authors.

References

1. Tanwar J, Das S, Fatima Z, et al. Multidrug resistance: an emerging crisis. Interdiscip Perspect Infect Dis 2014;2014:541340.

2. Antimicrobial Resistance C. Global burden of bacterial antimicrobial resistance in 2019: a systematic analysis. Lancet 2022;399:629-55.

3. Tacconelli E, Carrara E, Savoldi A, et al. Discovery, research, and development of new antibiotics: the WHO priority list of antibiotic-resistant bacteria and tuberculosis. Lancet Infect Dis 2018;18:318-27.

4. Kang CI, Kim SH, Kim HB, et al. Pseudomonas aeruginosa bacteremia: risk factors for mortality and influence of delayed receipt of effective antimicrobial therapy on clinical outcome. Clin Infect Dis 2003;37:745-51.

5. Moradali MF, Ghods S, Rehm BH. Pseudomonas aeruginosa Lifestyle: A Paradigm for Adaptation, Survival, and Persistence. Front Cell Infect Microbiol 2017;7:39.

6. Pang Z, Raudonis R, Glick BR, et al. Antibiotic resistance in Pseudomonas aeruginosa: mechanisms and alternative therapeutic strategies. Biotechnol Adv 2019;37:177-92.

[DOI: 10.22088/IJMCM.BUMS.13.1.46]

7. Yoshimura F, Nikaido H. Permeability of Pseudomonas aeruginosa outer membrane to hydrophilic solutes. J Bacteriol 1982;152:636-42.

8. Gellatly SL, Hancock RE. Pseudomonas aeruginosa: new insights into pathogenesis and host defenses. Pathog Dis 2013;67:159-73.

9. Alav I, Sutton JM, Rahman KM. Role of bacterial efflux pumps in biofilm formation. J Antimicrob Chemother 2018;73:2003-20.

10. Kishk RM, Abdalla MO, Hashish AA, et al. Efflux MexAB-Mediated Resistance in P. aeruginosa Isolated from Patients with Healthcare Associated Infections. Pathogens 2020;9.

11. Schweizer HP. Efflux as a mechanism of resistance to antimicrobials in Pseudomonas aeruginosa and related bacteria: unanswered questions. Genet Mol Res 2003;2:48-62.

12. Yoneyama H, Maseda H, Kamiguchi H, et al. Function of the membrane fusion protein, MexA, of the MexA, B-OprM efflux pump in Pseudomonas aeruginosa without an anchoring membrane. J Biol Chem 2000;275:4628-34.

13. Maurice NM, Bedi B, Sadikot RT. Pseudomonas aeruginosa Biofilms: Host Response and Clinical Implications in Lung Infections. Am J Respir Cell Mol Biol 2018;58:428-39.

14. Thi MTT, Wibowo D, Rehm BHA. Pseudomonas aeruginosa Biofilms. Int J Mol Sci 2020;21.

15. Khmel IA, Metlitskaya AZ. Quorum sensing regulation of gene expression: a promising target for drugs against bacterial pathogenicity. Mol Biol 2006;40:169-82.

16. Erickson DL, Endersby R, Kirkham A, et al. Pseudomonas aeruginosa quorum-sensing systems may control virulence factor expression in the lungs of patients with cystic fibrosis. Infect Immun 2002;70:1783-90.

17. Wang S, Feng Y, Han X, et al. Inhibition of Virulence Factors and Biofilm Formation by Wogonin Attenuates Pathogenicity of Pseudomonas aeruginosa PAO1 via Targeting pqs Quorum-Sensing System. Int J Mol Sci 2021;22.

18. Batoni G, Maisetta G, Esin S. Antimicrobial peptides and their interaction with biofilms of medically relevant bacteria. Biochim Biophys Acta 2016;1858:1044-60.

19. van Heuvel Y, Schatz S, Rosengarten JF, et al. Infectious RNA: Human Immunodeficiency Virus (HIV) Biology, Therapeutic Intervention, and the Quest for a Vaccine. Toxins (Basel) 2022;14.

20. Helbing CC, Hammond SA, Jackman SH, et al. Antimicrobial peptides from Rana [Lithobates] catesbeiana: Gene structure and bioinformatic identification of novel forms from tadpoles. Sci Rep 2019;9:1529.

21. Le CF, Fang CM, Sekaran SD. Intracellular Targeting Mechanisms by Antimicrobial Peptides. Antimicrob Agents Chemother 2017;61.

22. Huan Y, Kong Q, Mou H, et al. Antimicrobial Peptides: Classification, Design, Application and Research Progress in Multiple Fields. Front Microbiol 2020;11:582779.

23. Chen HL, Su PY, Chang YS, et al. Identification of a novel antimicrobial peptide from human hepatitis B virus core protein arginine-rich domain (ARD). PLoS Pathog 2013;9:e1003425.

24. Alves CS, Melo MN, Franquelim HG, et al. Escherichia coli cell surface perturbation and disruption induced by antimicrobial peptides BP100 and pepR. J Biol Chem 2010;285:27536-44.

25. Lamiable A, Thevenet P, Rey J, et al. PEP-FOLD3: faster de novo structure prediction for linear peptides in solution and in complex. Nucleic Acids Res 2016;44:W449-54.

26. Chen JE, Huang CC, Ferrin TE. RRDistMaps: a UCSF Chimera tool for viewing and comparing protein distance maps. Bioinformatics 2015;31:1484-6.

[DOI: 10.22088/IJMCM.BUMS.13.1.46]

27. Laskowski RA, MacArthur MW, Moss DS, et al. PROCHECK: a program to check the stereochemical quality of protein structures. J Appl Crystallogr 1993;26:283-91.

28. Wiederstein M, Sippl MJ. ProSA-web: interactive web service for the recognition of errors in three-dimensional structures of proteins. Nucleic Acids Res 2007;35:W407-10.

29. Waghu FH, Idicula-Thomas S. Collection of antimicrobial peptides database and its derivatives: Applications and beyond. Protein Sci 2020;29:36-42.

30. Gupta S, Kapoor P, Chaudhary K, et al. In silico approach for predicting toxicity of peptides and proteins. PLoS One 2013;8:e73957.

31. Pirtskhalava M, Amstrong AA, Grigolava M, et al. DBAASP v3: database of antimicrobial/cytotoxic activity and structure of peptides as a resource for development of new therapeutics. Nucleic Acids Res 2021;49:D288-D97.

32. Sharma A, Gupta P, Kumar R, et al. dPABBs: A Novel in silico Approach for Predicting and Designing Anti-biofilm Peptides. Sci Rep 2016;6:21839.

33. Vishnepolsky B, Pirtskhalava M. Prediction of linear cationic antimicrobial peptides based on characteristics responsible for their interaction with the membranes. J Chem Inf Model 2014;54:1512-23.

34. Gasteiger E, Gattiker A, Hoogland C, et al. ExPASy: The proteomics server for in-depth protein knowledge and analysis. Nucleic Acids Res 2003;31:3784-8.

35. Land H, Humble MS. YASARA: A Tool to Obtain Structural Guidance in Biocatalytic Investigations. Methods Mol Biol 2018;1685:43-67.

36. van Zundert GCP, Rodrigues J, Trellet M, et al. The HADDOCK2.2 Web Server: User-Friendly Integrative Modeling of Biomolecular Complexes. J Mol Biol 2016;428:720-5.

37. Honorato RV, Koukos PI, Jimenez-Garcia B, et al. Structural Biology in the Clouds: The WeNMR-EOSC Ecosystem. Front Mol Biosci 2021;8:729513.

38. Pawar SS, Rohane SH. Review on discovery studio: An important tool for molecular docking. Asian J Res Chem 2021; 14:86-8.

39. Laskowski RA, Jablonska J, Pravda L, et al. PDBsum: Structural summaries of PDB entries. Protein Sci 2018;27:129-34.

40. Balouiri M, Sadiki M, Ibnsouda SK. Methods for in vitro evaluating antimicrobial activity: A review. J Pharm Anal 2016; 6:71-9.

41. Macia MD, Rojo-Molinero E, Oliver A. Antimicrobial susceptibility testing in biofilm-growing bacteria. Clin Microbiol Infect 2014;20:981-90.

42. O'Toole GA, Kolter R. Flagellar and twitching motility are necessary for Pseudomonas aeruginosa biofilm development. Mol Microbiol 1998;30:295-304.

43. Wang CK, Shih LY, Chang KY. Large-Scale Analysis of Antimicrobial Activities in Relation to Amphipathicity and Charge Reveals Novel Characterization of Antimicrobial Peptides. Molecules 2017;22.

44. Giangaspero A, Sandri L, Tossi A. Amphipathic alpha helical antimicrobial peptides. Eur J Biochem 2001;268:5589-600.

45. Soukarieh F, Liu R, Romero M, et al. Hit Identification of New Potent PqsR Antagonists as Inhibitors of Quorum Sensing in Planktonic and Biofilm Grown Pseudomonas aeruginosa. Front Chem 2020;8:204.

46. Souza SGP, Santos ICD, Bondezan MAD, et al. Bacteria with a Potential for Multidrug Resistance in Hospital Material. Microb Drug Resist 2021;27:835-42.

[DOI: 10.22088/IJMCM.BUMS.13.1.46]

47. Hancock RE, Speert DP. Antibiotic resistance in Pseudomonas aeruginosa: mechanisms and impact on treatment. Drug Resist Updat 2000;3:247-55.

48. Drayton M, Kizhakkedathu JN, Straus SK. Towards Robust Delivery of Antimicrobial Peptides to Combat Bacterial Resistance. Molecules 2020;25.

49. Pinto SN, Dias SA, Cruz AF, et al. The mechanism of action of pepR, a viral-derived peptide, against Staphylococcus aureus biofilms. J Antimicrob Chemother 2019;74:2617-25.

50. Jung Y, Kong B, Moon S, et al. Envelope-deforming antiviral peptide derived from influenza virus M2 protein. Biochem Biophys Res Commun 2019;517:507-12.

51. Poorinmohammad N, Mohabatkar H, Behbahani M, et al. Computational prediction of anti HIV-1 peptides and in vitro evaluation of anti HIV-1 activity of HIV-1 P24-derived peptides. J Pept Sci 2015;21:10-6.

52. Sharma R, Shrivastava S, Kumar Singh S, et al. Deep-ABPpred: identifying antibacterial peptides in protein sequences using bidirectional LSTM with word2vec. Brief Bioinform 2021;22.

53. Cole AM, Liao HI, Ganz T, et al. Antibacterial activity of peptides derived from envelope glycoproteins of HIV-1. FEBS Lett 2003;535:195-9.

54. Dong M, Kwok SH, Humble JL, et al. BING, a novel antimicrobial peptide isolated from Japanese medaka plasma, targets bacterial envelope stress response by suppressing cpxR expression. Sci Rep 2021;11:12219.

55. Sakurai K, Yamasaki S, Nakao K, et al. Crystal structures of multidrug efflux pump MexB bound with high-molecular-mass compounds. Sci Rep 2019;9:4359.

56. Jafari P, Luscher A, Siriwardena T, et al. Antimicrobial Peptide Dendrimers and Quorum-Sensing Inhibitors in Formulating Next-Generation Anti-Infection Cell Therapy Dressings for Burns. Molecules 2021;26.

57. Mok N, Chan SY, Liu SY, et al. Vanillin inhibits PqsR-mediated virulence in Pseudomonas aeruginosa. Food Funct 2020;11:6496-508.

58. Ilangovan A, Fletcher M, Rampioni G, et al. Structural basis for native agonist and synthetic inhibitor recognition by the Pseudomonas aeruginosa quorum sensing regulator PqsR (MvfR). PLoS Pathog 2013;9:e1003508.

59. Hirt H, Gorr SU. Antimicrobial peptide GL13K is effective in reducing biofilms of Pseudomonas aeruginosa. Antimicrob Agents Chemother 2013;57:4903-10.

60. Kalaiselvan P, Kuppusamy R, Kumar N, et al. Antimicrobial activity of a peptide mimic against Pseudomonas aeruginosa in solution and when immobilised onto contact lenses. Invest Ophthalmol Vis Sci 2021;62:420-.

61. Li JF, Zhang JX, Li G, et al. Antimicrobial activity and mechanism of peptide CM4 against Pseudomonas aeruginosa. Food Funct 2020;11:7245-54.

62. Beaudoin T, Stone TA, Glibowicka M, et al. Activity of a novel antimicrobial peptide against Pseudomonas aeruginosa biofilms. Sci Rep 2018;8:14728.

63. Aflakian F, Rad M, Hashemitabar G, et al. Design and assessment of novel synthetic peptides to inhibit quorum sensing-dependent biofilm formation in Pseudomonas aeruginosa. Biofouling 2022;38:131-46.

64. Gopal R, Lee JH, Kim YG, et al. Anti-microbial, anti-biofilm activities and cell selectivity of the NRC-16 peptide derived from witch flounder, Glyptocephalus cynoglossus. Mar Drugs 2013;11:1836-52.

[DOI: 10.22088/IJMCM.BUMS.13.1.46]